

# Electronic Structure and Magnetic Exchange Interaction in Fe<sub>2</sub>NiAs Compound

XIAO-PING WEI<sup>a,\*</sup>, YA-LING ZHANG<sup>b</sup>, XIAO-WEI SUN<sup>a</sup>, TING SONG<sup>a</sup> AND XING-FENG ZHU<sup>c</sup>

<sup>a</sup>The School of Mathematics and Physics, Lanzhou Jiaotong University, Lanzhou 730070, P.R. China

<sup>b</sup>Institute of Modern Physics, Chinese Academy of Sciences, Lanzhou 730000, P.R. China

<sup>c</sup>Department of Physics, Nanjing Normal University, Nanjing 210023, P.R. China

(Received December 25, 2016; in final form June 24, 2017)

Using the spin-polarized relativistic Korringa–Kohn–Rostoker method, we study the electronic and magnetic properties of Fe<sub>2</sub>NiAs compound with the Hg<sub>2</sub>CuTi structure. Electronic calculations reveal the *d-d* orbital hybridization taking an important role in the compound. The calculated magnetic moments, which contain the spin and orbital moments, are primarily carried by Fe atoms located in A and B sites. The orbital moment of Fe<sub>2</sub>NiAs system is rather small due to the cause of orbital quenching, implying a weak spin–orbit coupling. Simultaneously, we also study the influence of lattice constant on the magnetic moment, it is found that both spin and orbital moments are sensitive to the changes of lattice constants, i.e., the moments become larger as the expansion of lattice constant, indicating the enhancement of spin–orbit coupling effect. In addition, we investigate the magnetic interactions between the constituents to obtain the Heisenberg exchange coupling parameters. It is noted that the interactions are dominated by a strong exchange between Fe atoms. Finally, we acquire the Curie temperatures of Fe<sub>2</sub>NiAs compound under different lattice constants by using mean field approximation.

DOI: [10.12693/APhysPolA.132.1320](https://doi.org/10.12693/APhysPolA.132.1320)

PACS/topics: 71.20.Lp, 71.20.Gj, 71.20.–b, 77.80.B–

## 1. Introduction

The Heusler compounds are a class of more than 1000 ternary intermetallic materials with composition X<sub>2</sub>YZ or XYZ, where X and Y are transition metals and Z is a main group element [1]. They usually crystallize in the *Fm* $\bar{3}$ *m* or *F* $\bar{4}$ *3m* space groups. In the two groups, various distributions of the X, Y, and Z elements among the specific crystallographic sites are possible [2], the physical properties of these compounds are strongly dependent on the distribution, and thus exhibiting a rich variety of physical properties [3]. For example, they can be used as metals, semiconductors, or superconductors. In addition, the different magnetic order between atoms, which ascribes to the different atomic distributions, leads to the various magnetic applications of these compounds. Such as they possess magnetic shape-memory characteristics, exhibit heavy-fermion behavior, have giant magnetoresistance and thermoelectric properties, etc. Some of these properties have great potential in semiconductor spintronic devices or magnetocaloric technology.

Fe<sub>2</sub>-based Heusler compounds, as a kind of the Heusler materials, have been predicted to be one of promising materials sources. Among them, Fe<sub>2</sub>NiZ alloys attend current widely interest from a theoretical and experimental points of view [4–8]. Fe<sub>2</sub>NiAs compound, as a subset of the Fe<sub>2</sub>Ni-based Heusler compounds, is of particular in semiconductor spintronics devices. However, some of conditions must be satisfied in realistic applications, e.g.,

it requires that Fe<sub>2</sub>NiAs must have the Curie temperature noticeably higher than the room temperature. Unfortunately, these data are still missing. In the literature, we study the electronic and magnetic properties of Fe<sub>2</sub>NiAs compound with Hg<sub>2</sub>CuTi structure, and then discuss the exchange interactions and the Curie temperature of Fe<sub>2</sub>NiAs compound.

## 2. Calculation details

We have performed the electronic structure calculations by using spin-polarized relativistic Korringa–Kohn–Rostoker code [9]. In this scheme, the exchange-correlation (XC) potential was adopted by the Vosko–Wilk–Nusair (VWN) within the local spin density approximation (LSDA) [10]. The self-consistent potentials were performed on 250 *k* points in the irreducible wedge of the Brillouin zone. The angular momentum expansion was taken up to  $l_{max} = 3$ . All calculations were carried out in the relativistic representation of the valence states, thus the spin–orbit coupling is taken into account.

In the classical Heisenberg model the Hamiltonian of a spin system is given by

$$H = - \sum_{i,j} e_i e_j J_{ij}, \quad (1)$$

where the  $J_{ij}$  is the Heisenberg pair exchange coupling parameters, and unit vectors  $e_i$  point to the direction of the magnetic moment on site  $i$ . The exchange coupling parameters can be obtained by mapping the system onto a Heisenberg Hamiltonian, and they are determined within a real-space approach using the theory by Liechtenstein et al. [11]. Based on the  $J_{ij}$ , the Curie temperatures were calculated within the mean field approximation (MFA). For a single-lattice system, the Curie

\*corresponding author; e-mail: [weixp2008@gmail.com](mailto:weixp2008@gmail.com)

temperature is given by

$$\frac{3}{2}\kappa_B T_C^{MFA} = J_0 = \sum_j J_{0j}. \quad (2)$$

In a multi-sublattice system, such as the  $\text{Fe}_2\text{NiAs}$  compound with four sublattices, one has to solve the following coupled equations:

$$\frac{3}{2}\kappa_B T_C^{MFA} \langle e^\nu \rangle = \sum_\nu J_0^{\mu\nu} \langle e^\nu \rangle, \quad (3)$$

$$J_0^{\mu\nu} = \sum_{r \neq 0} J_{0r}^{\mu\nu}, \quad (4)$$

where  $e^\nu$  is the average  $z$  component of the unit vector  $\langle e_r^\nu \rangle$  pointing in the direction of the magnetic moment at site  $(\nu, \mathbf{r})$ . Hence the coupled equations can be rewritten as an eigenvalue problem

$$(\Theta - T\mathbf{I})\mathbf{E} = 0, \quad (5)$$

$$\frac{3}{2}\kappa_B \Theta_{\mu\nu} = J_0^{\mu\nu}, \quad (6)$$

with a unit matrix  $\mathbf{I}$  and the vector  $e^\nu = \langle e_r^\nu \rangle$ . The largest eigenvalue of the  $\Theta$  matrix gives the Curie temperature [12]. The  $\mathbf{r}$ -summation in Eqs. (3),(4) was taken to a radius of  $r_{\max} = 3.0a$ , where  $a$  is the lattice constant.

### 3. Results and discussion

#### 3.1. Density of states

Prior to the presentation of our results, we have to shortly describe the  $\text{Hg}_2\text{CuTi}$  structure, which consists of four interpenetrating fcc lattices, i.e., A  $(0,0,0)$ , B  $(\frac{1}{4}, \frac{1}{4}, \frac{1}{4})$ , C  $(\frac{1}{2}, \frac{1}{2}, \frac{1}{2})$  and D  $(\frac{3}{4}, \frac{3}{4}, \frac{3}{4})$  sites, one of them is shifted by the vector  $(\frac{1}{4}, \frac{1}{4}, \frac{1}{4})$  [13]. Among them, the A and B sites are occupied by the Fe atoms, and the C and D sites are occupied by Ni and As atoms. This occupation is preferred with respect to the Heusler structure if X has less valence electrons than Y [14, 15]. In this structure, the inversion symmetry is broken and it is thus assigned to space group  $F\bar{4}3m$ . It can be viewed as a generalization of the Heusler structure. Just as most semiconductors crystallizing in this structure, thus it is of technological importance as an injection source of spin-polarized electrons. To obtain the equilibrium state of  $\text{Fe}_2\text{NiAs}$  compound, we fit first the curve of energy-volume by using the Murnaghan equation [16], the results show the ground state of  $\text{Fe}_2\text{NiAs}$  has a lattice parameter of 5.531 Å, which matches well with most conventional semiconductors, thus it is more suitable for semiconductor spintronics application. Moreover, the electronic and magnetic properties are calculated based on the equilibrium state.

The spin-polarized total, atomic and orbital-resolved density of states (DOS) of  $\text{Fe}_2\text{NiAs}$  in the ferromagnetic state are shown in Fig. 1. It is apparent that the DOS around the Fermi level ( $E_F$ ) is dominated by the Fe- and Ni- $d$  states. For the spin-up configuration, these states are spread in the energy region from about  $-5$  to  $1$  eV. However, for the spin-down configuration, these states are spread between about  $-6$  to  $0.5$  eV with respect to  $E_F$ . More noticeably, the  $d$ -states are more distributed

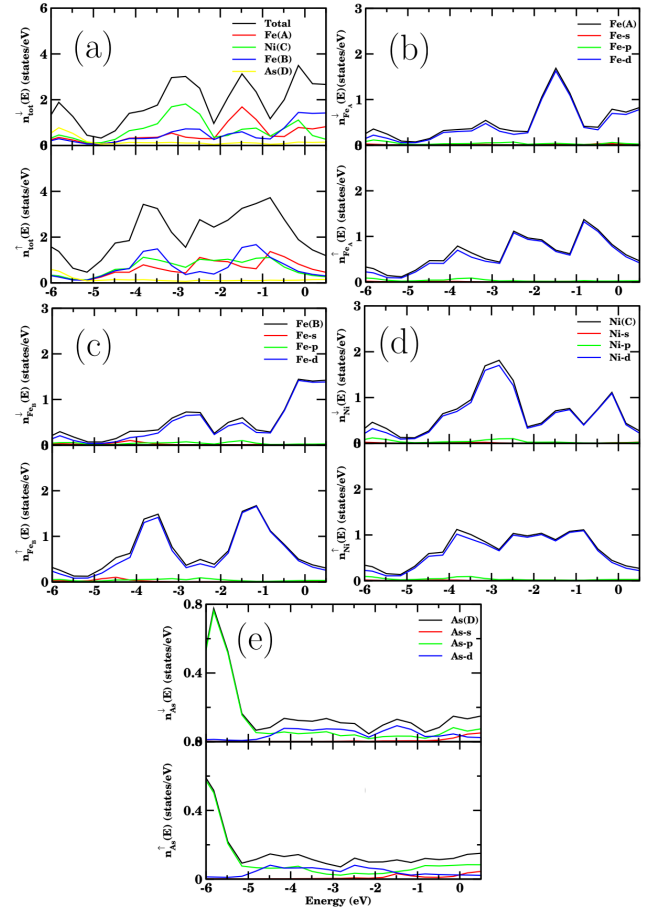


Fig. 1. Spin-polarized total, atomic, and orbital-resolved density of states of  $\text{Fe}_2\text{NiAs}$  in the ferromagnetic state.

in spin-up channel at the  $E_F$  than that of spin-down, thus resulting in a high spin-polarization, it is favorable for spintronics applications. One also observe that the  $d$  states of Fe atoms from the A and B sites are the main contribution to the DOS. Regarding the spin-up configuration, the Fe(A)- $d$  states are widely spread from  $-4.5$  to  $0.5$  eV and are highly peaked at about  $-0.7$  and  $-2.5$  eV. The Fe(B)- $d$  states, however, are strongly peaked at about  $-3.5$  and  $-1.2$  eV. In the case of spin-down configuration, the Fe(A)- $d$  states occupy a region from  $-4.5$  to  $0.5$  eV in energy and are strongly peaked in the vicinity of  $-1.5$  eV, while for Fe(B)- $d$  states the stronger peaks are distributed around the  $E_F$ . In contrast, the DOS arising from the Ni- $d$  state is different from that of the Fe- $d$  states since the contributions from spin-up and spin-down configurations below the  $E_F$  are of almost the same weight, thus there is smaller magnetic moment than Fe atoms. However, for the spin-down configuration, the dominant contribution of the Ni- $d$  states is peaked at about  $-3$  eV below  $E_F$ . The separation of spin-up and spin-down DOS for Fe and Ni leads to nonzero Fe and Ni magnetic moments, this is also a direct result of the unfilled  $3d$  shells in both atoms. In addition, we can see from the DOS in Fig. 1, the contribution of As to the overall DOS is

negligibly small, most notably, the states in both spin-up and spin-down configurations are distributed in a similar way, thus resulting in the value of As magnetic moment is close to zero.

### 3.2. Magnetic moments

Spin and orbital magnetic moments of  $\text{Fe}_2\text{NiAs}$  compound are tabulated in Table I, respectively. It can be seen the spin and orbital moments are carried by Fe atoms, the value of spin moment is  $1.1574 \mu_B$  for Fe(A) atom, while for Fe(B) atom, it is  $2.0180 \mu_B$ . The fact is the magnetic moment of Fe(B) atom is larger than that of Fe(A) atom, the result can be deduced by inspecting Fig. 1, namely, the distribution of the spin-up Fe(B)- $d$  states is larger than that of the spin-up Fe(A)- $d$  states. The total spin and orbital magnetic moment per formula is  $3.1939$  and  $0.0995 \mu_B$ , indicating a weak effect of spin-orbit coupling. Further, we discuss the total and site resolved magnetic moments under different lattice constants.

TABLE I

Spin and orbital magnetic moments (in  $\mu_B$  unit) of  $\text{Fe}_2\text{NiAs}$  compound.

	Total	Fe(A)	Fe(B)	Ni(C)	As(D)
spin	3.1939	1.1574	2.0180	0.0348	-0.0163
orbit	0.0994	0.0274	0.0632	0.0079	0.0008

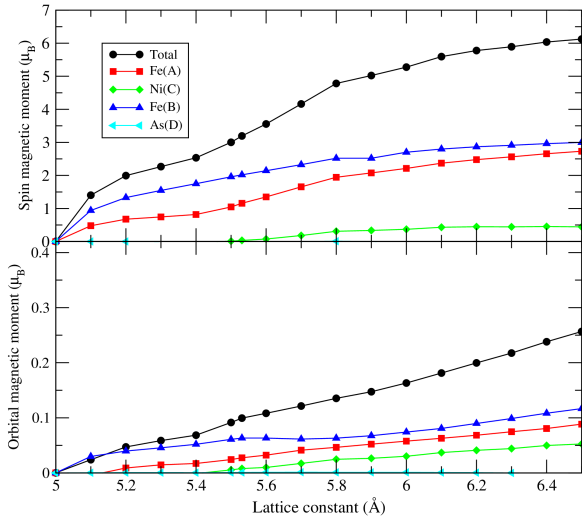


Fig. 2. Dependences of spin and orbital magnetic moments on lattice parameter in  $\text{Fe}_2\text{NiAs}$ .

In Fig. 2, we show the changes of magnetic moments with lattice constants. It is found that total magnetic moment is enlarged as the expansion of lattice constants, the change attributes to the improvement of Fe and Ni atomic moments. Only small changes are observed for the site resolved moments for As atom, implying the As atom nearly unpolarized. The changes of the Fe and Ni moments can be traced to the increase of lattice parameter. As the expansion of lattice parameter, the orbital

overlap is reduced, and then leading to weaker hybridizations between atoms. Due to the reduction of itinerancy, the quenching of the atomic moments become invalid and the moments become more atomic-like, i.e., larger.

### 3.3. Exchange interactions and Curie temperatures

In Fig. 3, we show the calculated Heisenberg exchange coupling parameters. It is evident that the exchange interactions are tightly restricted to clusters of radius  $r \leq 2.0a$ . Specifically, the inter-sublattice Fe(A)-Fe(B) interaction provides significant contribution in interactions, while the intra-sublattice contributions are mainly from Fe(A)-Fe(A) and Fe(B)-Fe(B) interactions. It should be kept in mind that among the dominating interactions the Fe(A)-Fe(B) interaction is the strongest one, and decide the magnitude of the Curie temperature to some extent. In contrast, the Ni(C)-Fe(A), Ni(C)-Fe(B) and Ni(C)-Ni(C) interactions are much weaker. In detail, it notices that the first and second nearest neighbors interactions indicate the antiferromagnetic coupling for inter-sublattice Fe(A)-Fe(B) interaction, while for the intra-sublattice Fe(A)-Fe(A) and Fe(B)-Fe(B) interactions, the  $J_{ij}$  shows a oscillation behavior as the increase of interatomic distance  $r$ , and finally the behavior disappears with increase of interatomic distance, indicating a long-ranged Ruderman-Kittel-Kasuya-Yosida (RKKY)-like behavior. Generally, a negative  $J_{ij}$  implies that the interaction acts against the ferromagnetic order on this lattice and reduces the Curie temperature. By contrast, a positive  $J_{ij}$  can improve the Curie temperature. In addition, the interactions with As are omitted, because it is close to the zero for all distances.

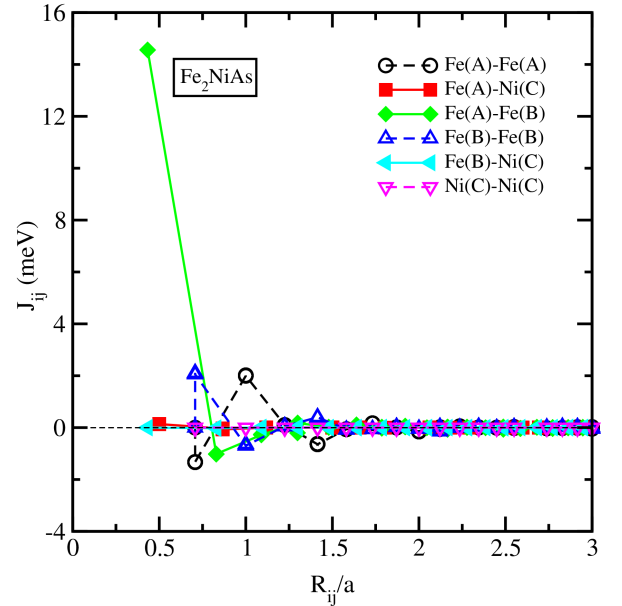


Fig. 3. Heisenberg exchange coupling parameters  $J_{ij}$  for the  $\text{Fe}_2\text{NiAs}$  compound as a function of the interatomic distance  $r$ . Note that the solid lines represent inter-sublattice interactions, and the dotted lines represent intra-sublattice interactions.

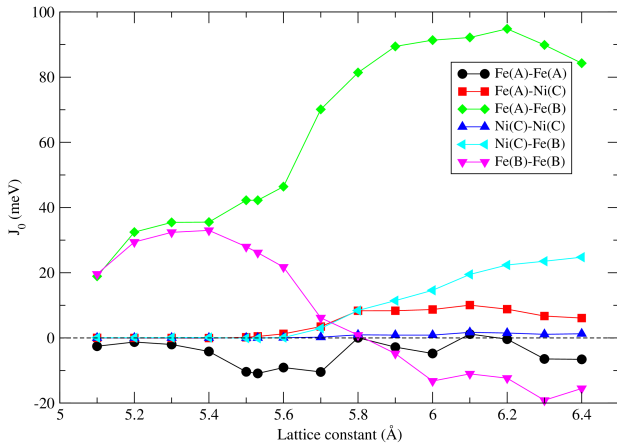


Fig. 4. Dependences of exchange coupling parameters  $J_0$  on different lattice constants in  $\text{Fe}_2\text{NiAs}$  compound.

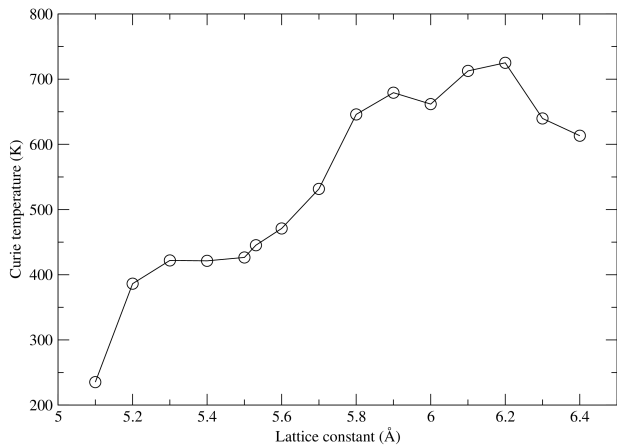


Fig. 5. Changes of Curie temperature with the lattice constants.

In Fig. 4 the relevant contributions to the  $J_0$  matrix on the lattice constants are displayed. It can be seen that the inter-sublattice Fe(A)-Fe(B) exchange offers a major contribution in interactions, and are roughly proportional to the changes of Fe magnetic moments. The increase of Fe magnetic moment enhances the  $J_0$  of intra-sublattice Ni-Fe exchange. For the  $J_0$  of intra-sublattice Fe(B)-Fe(B) exchange, a decreased tendency is shown, implying the reduction of direct exchange interaction. The interactions of intra-sublattice Ni(C)-Ni(C) almost have no contribution to overall interactions since the Ni magnetic moment almost keep the constant at different lattice constants. Essentially, the  $J_0$  is decided by the atomic magnetic moment under different lattice constants.

From the exchange coupling parameters described above, we calculate the Curie temperature by the mean field approximation. It is found that the Curie temperature at equilibrium is up to 445.25 K, which is higher than the room temperature, indicating its potential magnetic applications.

In addition, we show the dependence of the Curie temperature on the lattice parameters in Fig. 5, which helps

us to identify the changes of sum of exchange interactions, it is obvious that the Curie temperature is higher than the room temperature above the 5.2 Å, even reaching almost 725 K at 6.2 Å, it is favorable in realistic applications. For the jump of the Curie temperature at 6.0 Å, the Fe(B)-Fe(B) exchange interaction can explain the unexpected behaviour. It should be noted that the Curie temperature of  $\text{Fe}_2\text{NiAs}$  compound is roughly proportional to the total spin moment. On the other hand, the site resolved magnetic moments change considerably with the enlarge of lattice parameter (see Fig. 2), and then leading to larger exchange interactions.

#### 4. Summary and conclusions

We have performed the electronic and magnetic calculations on the  $\text{Fe}_2\text{NiAs}$  compound with the  $\text{Hg}_2\text{CuTi}$  structure by using the full potential Korringa-Kohn-Rostoker method. The DOS show that Fe- and Ni- $d$  states dominate the Fermi level and determine the electronic properties, the contribution of As is negligibly small to total DOS. Simultaneously, the separation of spin-up and spin-down DOS leads to nonzero Fe and Ni magnetic moments. This is a direct result of the unfilled  $3d$  shells in both atoms, while for As atom, the states in both configurations are distributed in a similar way, resulting that the value of the As magnetic moment is close to zero. As the expansion of lattice parameters, the magnetic moments become more larger due to the reduction of atomic orbital overlap. Further, we calculate the exchange interaction parameters under lattice constants, it is found that Fe(A)-Fe(B) exchange plays a leading role in interactions. Finally, the Curie temperatures are calculated by using the mean-field approximation. Results indicate the Curie temperatures are higher than the room temperature above 5.2 Å, which is favorable in realistic applications. More noticeably, the Curie temperatures show an anomalous dependence on the total moment, i.e., the Curie temperature enlarges as the expansion of lattice parameters, even reaching almost 725 K at 6.2 Å. Due to the loss of other data, no systematic comparison can be made. Therefore, we hope that the study can provide some valuable hints for further experimental and theoretical investigations.

#### Acknowledgments

The Project is supported by the Young Scholars Science Foundation of Lanzhou Jiaotong University (No. 2015028). This work is also supported by National Natural Science Foundation of China (No. 11647151) and the Scientific Research Project of Gansu Province (No. 2016-B029). Discussions with Markus Meinert are gratefully acknowledged.

#### References

- [1] T. Graf, J. Winterlik, L. MÜchler, G.H. Fecher, C. Felser, S.S.P. Parkin, in: *Handbook of Magnetic Materials*, Vol. 21, Ed. K.H.J. Buschow, Elsevier, Amsterdam 2013, p. 1.
- [2] G.E. Bacon, J.S. Plant, *J. Phys. F* **1**, 524 (1971).

- [3] T. Graf, C. Felser, S.S.P. Parkin, *Prog. Solid State Chem.* **39**, 1 (2011).
- [4] F. Nejdassattari, Z.M. Stadnik, J. Przewoźnik, K.H.J. Buschow, *Physica B* **477**, 113 (2015).
- [5] Y.J. Zhang, W.H. Wang, H.G. Zhang, E.K. Liu, R.S. Ma, G.H. Wu, *Physica B* **420**, 86 (2013).
- [6] D.C. Gupta, I.H. Bhat, *Mater. Chem. Phys.* **146**, 303 (2014).
- [7] T. Gasi, V. Ksenofontov, J. Kiss, S. Chadov, A.K. Nayak, M. Nicklas, J. Winterlik, M. Schwall, P. Klaer, P. Adler, C. Felser, *Phys. Rev. B* **87**, 064411 (2013).
- [8] Ming Yin, P. Nash, Song Chen, *Intermetallics* **57**, 34 (2015).
- [9] H. Ebert, D. Ködderitzsch, J. Minár, *Rep. Prog. Phys.* **74**, 096501 (2011).
- [10] S.H. Vosko, L. Wilk, M. Nusair, *Can. J. Phys.* **58**, 1200 (1980).
- [11] A.I. Liechtenstein, M.I. Katsnelson, V.P. Antropov, V.A. Gubanov, *J. Magn. Magn. Mater.* **67**, 65 (1987).
- [12] E. Şaşıoğlu, L.M. Sandratskii, P. Bruno, *J. Phys. Condens. Matter* **17**, 995 (2005).
- [13] X.P. Wei, Y.D. Chu, X.W. Sun, T. Sun, P. Guo, *Physica B* **463**, 103 (2015).
- [14] H.C. Kandpal, G.H. Fecher, C. Felser, *J. Phys. D Appl. Phys.* **40**, 1507 (2007).
- [15] H.Z. Luo, Z.Y. Zhu, L. Ma, S.F. Xu, X.X. Zhu, C.B. Jiang, H.B. Xu, G.H. Wu, *J. Phys. D Appl. Phys.* **41**, 055010 (2008).
- [16] F.D. Murnaghan, *Finite Deformation of an Elastic Solid*, Dover, New York 1967.